

# Substituent Effect on the Meso-Substituted Porphyrins: Theoretical Screening of Sensitizer Candidates for Dye-Sensitized Solar Cells

Ruimin Ma,<sup>†</sup> Ping Guo,<sup>†</sup> Hongji Cui,<sup>†</sup> Xianxi Zhang,<sup>\*,†,‡</sup> Mohammad K. Nazeeruddin,<sup>\*,‡</sup> and Michael Grätzel<sup>\*,‡</sup>

School of Chemistry and Chemical Engineering, Liaocheng University, Liaocheng 252059, China, and Laboratory for Photonics and Interfaces, Swiss Federal Institute of Technology, CH 1015, Lausanne, Switzerland

Received: June 9, 2009; Revised Manuscript Received: August 1, 2009

According to the concepts of attribute axis and attribute coordinate system, porphine and 11 kinds of bridge carbon substituted porphyrins as donors and 9 common acceptors A–I have been designed and calculated at the density functional B3LYP level. The substituent effects on the molecular orbital energy levels of the porphyrin derivatives have been discussed and promising donor–acceptor combinations are screened. Several novel zinc metalloporphyrins selected were then calculated by means of the DFT/TDDFT method in THF solvent. The electronic and spectroscopic properties of ZnTPP and the selected novel zinc porphyrin complexes have been investigated as solar cell sensitizers. The results show that the candidates selected are very promising to provide good performances as sensitizers, in which ZnTPPG is promising to challenge the current photoelectric conversion efficiency record 7.1% of porphyrin-sensitized solar cells. The concepts of attribute axis and attribute coordinate system are shown very helpful for tuning the molecular properties and the rational design of functional molecules with anticipated good properties.

## 1. Introduction

Dye-sensitized solar cells (DSSCs) have attracted significant attention as low-cost alternative to the conventional solid-state photovoltaic devices.<sup>1–6</sup> The most successful sensitizers employed in these cells are polypyridylruthenium complexes, which yield photon-to-current power conversion efficiencies of 10–11% with simulated sunlight.<sup>2,6</sup> However, ruthenium is not readily available. The complexes derived from metals that are common in nature or the free-metal compounds become more and more important, in which porphyrin dyes play an important role.<sup>7–16</sup>

Porphyrins exhibit long-lived (>1 ns)  $\pi^*$  singlet excited states and only weak singlet/triplet mixing. They have appropriate lowest unoccupied molecular orbital (LUMO) levels that reside above the conduction band of the  $\text{TiO}_2$  and highest occupied molecular orbital (HOMO) levels that lie below the redox couple in the electrolyte solution, required for charge separation at the semiconductor/dye/electrolyte surface, which makes them good donor moieties.<sup>7,17</sup> They mostly have broad photovoltaic responding band (between 400 and 650 nm) due to  $\pi$ – $\pi^*$  transitions of the conjugated macrocycle.<sup>10</sup> Significantly, the porphyrin dyes show comparatively high molar extinction coefficients, for example,  $\epsilon = 18\,500\text{ cm}^{-1}\text{ M}^{-1}$  at  $\lambda_{\text{max}} = 622\text{ nm}$ , suggesting that further optimization of this family may be a fruitful source of novel long-wavelength-absorbing dyes.<sup>3</sup> Since the conversion efficiencies of porphyrin-sensitized solar cells are still not high enough, it is thus very important to tune the molecular orbital energy levels and further the light absorption properties of these compounds to get higher conversion efficiency.

The side chains and the peripheral hydrogen atoms of the porphyrin compounds are easy to be modified. Design and synthesis

of many kinds of the porphyrin model compounds to further increase the photoelectricity conversion efficiency has attracted a great deal of attention.<sup>7–10</sup> However, the knowledge of the substituent effect is still not systematic and the use of the substituents to modify and design functional molecules is still empirical and random. Balanay et al.<sup>17</sup> found that the electron-donating substituents have almost no influence on the HOMO and LUMO levels in both free-base and zinc porphyrins; however, they checked a few substituents only, which may make the conclusion limited. It is thus very important to find a way to systematically master the substituent effects and rationally use them to modify and design molecules with anticipated properties.

According to our concept of attribute axis,<sup>18</sup> we believe that the electron-withdrawing or -donating abilities of various substituents are different and they can be lined up from weak to strong along an axis, which is the electron-withdrawing or -donating ability axis herein. The scope of this axis is unlimited, in which any group or molecular fragment can find its own place according to its electron-withdrawing or -donating ability. With these different substituents being connected with the parent molecule, a series of derivatives will be created and their various properties will vary systematically in certain ranges, which can be lined up along corresponding attribute axes. The term *attribute* here may indicate any property of molecules. These corresponding attribute axes combine together with the electron-withdrawing or -donating ability axis will form corresponding attribute coordinate systems,<sup>18</sup> in which each compound has its own coordinates. Since the scopes of each axis are unlimited, designs can be provided as many as possible, from which promising candidates with anticipated properties may be screened. Assisted with these attribute coordinate systems, with wider range of the electron-withdrawing or -donating substituents along the axis being checked, the way may be found to tune the molecular orbital energy levels of porphyrins.

Most of the efficient sensitizers have donor and acceptor moieties, between which there are sometimes  $\pi$  conjugation

\* Corresponding author. Tel.: +86 635 8230680. Fax: +86 635 8239121. E-mail: zhangxianxi@lcu.edu.cn.

<sup>†</sup> Liaocheng University.

<sup>‡</sup> Swiss Federal Institute of Technology.

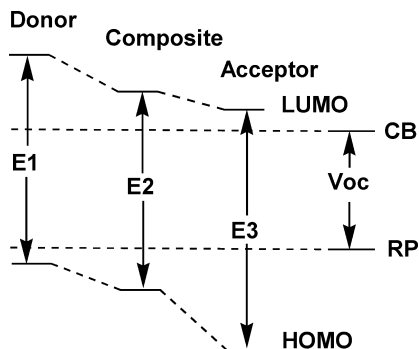


**Figure 1.** Orbital energy levels of the donor, acceptor and the composite sensitizer (CB, conduction band of the semiconductor; RP, redox potential of the electrolyte).

moieties. An anchoring group, typically the carboxyl or the phosphonic acid group, is connected to the acceptor group to inject the photoexcited electrons into the conduction band of the semiconductor. An oriented electron transfer from the donor moiety to the acceptor moiety is preferred for the efficient electron injection. That is to say, the HOMO of the sensitizer should be mainly localized at the donor part and the LUMO at the acceptor part. It is thus necessary to tune the donor and the acceptor moieties separately for finely tuning of the whole sensitizer.

The HOMO and LUMO energy levels of the composite molecule depend on the HOMO and the LUMO energy levels of the donor and the acceptor moieties, as shown in Figure 1. The HOMO level of the donor moiety should be higher than that of the acceptor moiety. As we know, the electrons at higher energy orbital are easily excited. When such a donor and acceptor form the composite sensitizer molecule, the HOMO will be mainly localized at the donor part. Similarly, the LUMO of the acceptor should be lower than that of the donor part. The excited electrons prefer to enter an unoccupied orbital with a lower energy level. When such a donor and acceptor form the composite sensitizer molecule, the LUMO will be mainly localized at the acceptor part. If the LUMO of the donor moiety is lower than that of the acceptor moiety, the electrons will be transferred to the donor, which cannot be injected into the semiconductor. If the HOMO of the acceptor is higher than that of the donor, then the electrons will be transferred from the acceptor, in which case the donor does not contribute much to the electron transfer. An oriented electron transfer can thus be controlled. And thus we can find out in advance if promising electron transfer can be obtained by the calculation and comparison of the separated donor and acceptor moieties rather than the much larger composite molecules. Of course this is only a simple analysis based on the HOMO and the LUMO. For further detailed analysis, the next several highest occupied orbitals and lowest unoccupied orbitals should also be considered.

Such molecule tuning concepts are used in the current study of the porphyrin sensitizers. The porphyrin moiety is considered as the donor and the long chain with the final carboxyl group is considered as the acceptor. Since the conjugation from the porphyrin macrocycle to the acceptor occurs more easily at the  $\beta$ -position,<sup>7</sup> we therefore prefer to study the substituent effect at the meso-positions, with the  $\beta$ -positions ( $-R$ ) left for future connection of the acceptor. Porphine and 11 kinds of porphyrins substituted at the meso-positions with substituents of different electron-withdrawing or -donating abilities, namely  $-\text{CH}_3$ ,  $-\text{OH}$ ,  $-\text{SH}$ ,  $-\text{CCH}$ ,  $-\text{F}$ ,  $-\text{Cl}$ ,  $-\text{Br}$ ,  $-\text{Ph}$ ,  $-\text{COOH}$ ,  $-\text{CN}$  and  $-\text{NH}_2$  (Figure 2), were studied through density functional B3LYP/6-31G(d) calculations using the Gaussian03 program.<sup>19</sup>

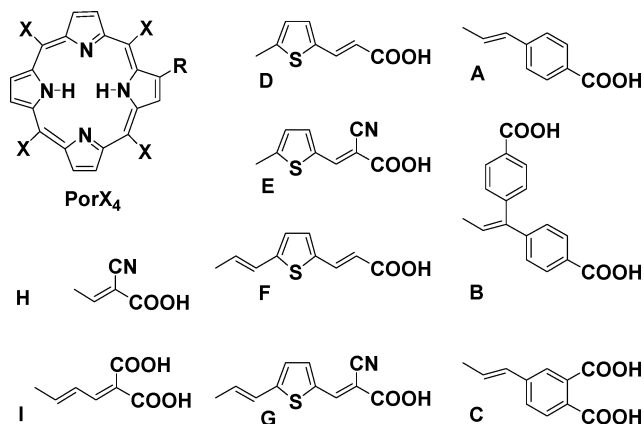


**Figure 2.** Structures of porphyrin donors ( $X = \text{H}, -\text{CH}_3, -\text{OH}, -\text{SH}, -\text{CCH}, -\text{F}, -\text{Cl}, -\text{Br}, -\text{Ph}, -\text{COOH}, -\text{CN}$  and  $-\text{NH}_2$ ) and acceptors.

The orbital energy levels of nine common acceptors A–I (Figure 2) were also calculated using the same method and compared with those of the porphyrin donors. Some promising combinations of donors and acceptors were found for further sensitizer candidates design.

After the initial calculations of the separated donor and acceptor moieties, the most commonly used donor tetraphenylporphyrin (TPP) and several preferable acceptors were paired together to construct the final sensitizers as the first series of sample candidates. Considering the influences of the central ions, the two central  $\text{H}^+$  ions were replaced by  $\text{Zn}^{2+}$  ions. The combinations of the other donors and acceptors will be reported later in another paper considering the clarity and the length limit of the current paper.

## 2. Computational Method

Hydrogen and eleven kinds of substituents along the electron-donating and -withdrawing ability axis including both electron-donating and electron-withdrawing ones, namely  $-\text{CH}_3$ ,  $-\text{OH}$ ,  $-\text{SH}$ ,  $-\text{CCH}$ ,  $-\text{F}$ ,  $-\text{Cl}$ ,  $-\text{Br}$ ,  $-\text{Ph}$ ,  $-\text{COOH}$ ,  $-\text{CN}$  and  $-\text{NH}_2$ , are chosen to substitute at the bridge carbon positions of the porphyrin. These porphyrins together with nine kinds of acceptor moieties A–I (Figure 2) were calculated at density functional B3LYP level using the 6-31G(d) basis set for both geometry optimizations and frequency calculations. The orbital energy levels of the porphyrin donors and the acceptors were compared to screen appropriate donor–acceptor pairs for further zinc metalloporphyrin sensitizer candidates design.

Since the optimization of the zinc porphyrin complexes using the B3LYP exchange–correlation functional and 6-31G(d) basis set was difficult to obtain, the LANL2DZ basis set was used instead for further calculations of ZnTPP and the selected zinc metalloporphyrins. The electronic absorption spectra of the selected zinc metalloporphyrins were calculated and simulated with the time-dependent density functional theory (TDDFT) method in THF solvent, which was used in previous experimental works. All calculations were carried out using the Gaussian03 program<sup>19</sup> on the IBM P690 system in Shangdong Province High Performance Computer Center.

## 3. Results and Discussion

**3.1. Molecular Orbital Energy Levels of the Donor and Acceptor Moieties.** The LUMO and HOMO orbital energy graphs of differently substituted porphyrins are shown in Figure 3, and corresponding data are listed in Table 1 together with

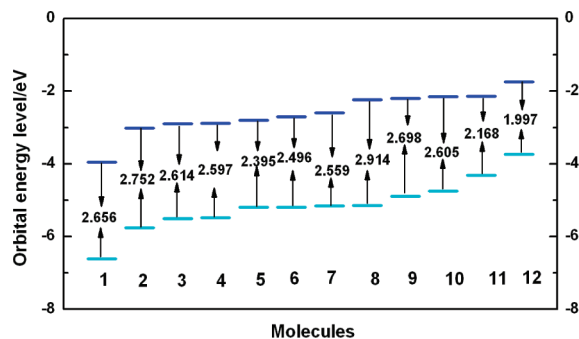


**Figure 3.** Orbital energy levels of the HOMO and LUMO and the HOMO–LUMO gaps of  $\text{H}_2\text{Por}(\text{CN})_4$  (1),  $\text{H}_2\text{Por}(\text{COOH})_4$  (2),  $\text{H}_2\text{PorCl}_4$  (3),  $\text{H}_2\text{PorBr}_4$  (4),  $\text{H}_2\text{Por}(\text{CCH})_4$  (5),  $\text{H}_2\text{Por}(\text{SH})_4$  (6),  $\text{H}_2\text{PorF}_4$  (7),  $\text{H}_2\text{Por}$  (8),  $\text{H}_2\text{Por}(\text{Ph})_4$  (9),  $\text{H}_2\text{Por}(\text{CH}_3)_4$  (10),  $\text{H}_2\text{Por}(\text{OH})_4$  (11), and  $\text{H}_2\text{Por}(\text{NH}_2)_4$  (12).

**TABLE 1: LUMO and HOMO Energy Levels of Porphyrin Donors and Acceptors A–I (eV)**

molecule	$\epsilon_{\text{LUMO}}$	$\epsilon_{\text{HOMO}}$	molecule	$\epsilon_{\text{LUMO}}$	$\epsilon_{\text{HOMO}}$
$\text{H}_2\text{Por}(\text{NH}_2)_4$	−1.746	−3.743	$\text{H}_2\text{Por}(\text{CN})_4$	−3.959	−6.615
$\text{H}_2\text{Por}(\text{OH})_4$	−2.147	−4.315	A	−1.705	−6.410
$\text{H}_2\text{Por}(\text{CH}_3)_4$	−2.149	−4.754	B	−1.821	−6.431
$\text{H}_2\text{PorPh}_4$	−2.201	−4.899	C	−1.915	−6.569
$\text{H}_2\text{Por}$	−2.234	−5.148	D	−1.991	−6.212
$\text{H}_2\text{PorF}_4$	−2.601	−5.160	F	−2.180	−5.834
$\text{H}_2\text{Por}(\text{SH})_4$	−2.700	−5.197	I	−2.241	−7.010
$\text{H}_2\text{Por}(\text{CCH})_4$	−2.802	−5.197	H	−2.463	−8.226
$\text{H}_2\text{PorBr}_4$	−2.887	−5.484	E	−2.680	−6.621
$\text{H}_2\text{PorCl}_4$	−2.898	−5.512	G	−2.829	−6.233
$\text{H}_2\text{Por}(\text{COOH})_4$	−3.017	−5.768			

those of the acceptors A–I. This table and figure can both be considered as representations of the attribute coordinate systems formed by the molecular orbital energy level axis and the electron-withdrawing or -donating ability axis. It can be noted from them that the molecular orbital energy levels of the porphyrin derivatives, especially HOMO and LUMO, vary systematically from low to high along the variation of the substituents from electron-withdrawing to electron-donating, which display clearly the relationship between the molecular orbital energy levels of the porphyrin derivatives and the substituents to be used.

The typical porphyrins used as sensitizers in DSSCs mostly have porphyrin moieties as donors and carboxyl-containing groups as acceptors, which anchor the dyes onto the  $\text{TiO}_2$  surface.<sup>8</sup> The charge transfer orientation is associated with the difference between the HOMO of the donor and the LUMO of the acceptor, which is an important factor that affects the electron injection efficiency. The LUMO is localized in the acceptor region and the HOMO in the donor region when the difference between  $\text{LUMO}_{\text{donor}}$  and  $\text{LUMO}_{\text{acceptor}}$  is positive,<sup>17</sup> which is indicative of a charge-separated state. The donor should have the higher HOMO and LUMO energy levels compared to the acceptor as discussed above; therefore, the HOMO of the whole molecule will be dominated by the HOMO of the donor and the LUMO will be dominated by the LUMO of the acceptor. When the donor absorbs light energy, it injects an electron into the LUMO of the acceptor, which then injects it into the conduction band of  $\text{TiO}_2$ .

The porphyrins should be connected with acceptors that match them well. Since a  $\text{LUMO}_{\text{donor}} - \text{LUMO}_{\text{acceptor}}$  difference ranging from 0.10 to 0.20 eV was considered sufficient for charge transport,<sup>17</sup> it is thus easy to pick up the appropriate donor–acceptor combinations. As shown in Table 1, the LUMO energy

level of  $-\text{NH}_2$  substituted porphyrin is higher than those of acceptors C, D, F, I, H, E, and G. Those of  $-\text{OH}$ ,  $-\text{CH}_3$  and  $-\text{Ph}$  substituted compounds as well as porphine are higher than those of acceptors H, E, G, and I may also be considered since they play an important role in the best porphyrin sensitizer reported until now.<sup>16</sup> And those of  $-\text{F}$  and  $-\text{SH}$  substituted porphyrins are higher than the acceptor G. These donors and acceptors may thus form good donor–acceptor pairs.

The most commonly used tetraphenylporphyrin ( $\text{H}_2\text{TPP}$ ) donor and several preferable acceptors were paired together to construct the final sensitizers as the first series of sample candidates. Considering the influences of the central ions, the two central  $\text{H}^+$  ions were replaced by  $\text{Zn}^{2+}$  ions ( $\text{ZnTPP}$ ). The combinations of the other donors and acceptors will be reported later in another paper considering the clarity and the length limit of the current paper.

**3.2. Electronic Structures of the Selected Zinc Porphyrin Sensitizer Candidates.** According to the discussion above, the structures of  $\text{ZnTPP}$  and the selected zinc metalloporphyrins were investigated at the density functional B3LYP level using the LANL2DZ basis set for both geometry optimization and frequency calculation. No imaginary vibration was predicted in the frequency calculations, indicating that the energy minimum structures of all the selected zinc metalloporphyrins are true energy minima. Mizuseki et al.<sup>20</sup> suggested that the charge transport was also related to the spatial distribution and the composition of the frontier orbital. To get more information about these molecules, the composition and spatial distribution of the HOMO and LUMO for  $\text{ZnTPP}$  and these zinc metalloporphyrins selected were also calculated. Campbell et al.<sup>16</sup> have reported the conversion efficiency 7.1% of zinc tetra-4-methylphenylporphyrin ( $\text{ZnTMPP}$ ) as donor combined with acceptor I, which is the best porphyrin sensitizer up to now. So the  $\text{ZnTMPP}$  compound was also calculated as a reference.

The orbital spatial distributions of HOMO and LUMO for  $\text{ZnTPP}$  and the zinc metalloporphyrins selected are shown in Figure 4. It is obvious that the HOMO and LUMO of  $\text{ZnTPP}$  both localize at the central porphyrin ring, which is not good for forming the electron-separated state. The HOMOs of the zinc metalloporphyrins selected are mainly localized at the central porphyrin ring; however, the LUMOs are much more localized at the carboxyl-containing substituents, which indicates a good electron-separated state. This corresponds well with the anticipation from the analysis of the separated donor and acceptor moieties.

The compositions of the HOMO and LUMO for  $\text{ZnTPP}$  and the zinc metalloporphyrins selected are shown in Table 2. The HOMO of  $\text{ZnTPPA}$  is mainly composed of  $\text{ZnTPP}$ , while for the LUMO the contribution of A is obviously increased.  $\text{ZnTPPH}$ ,  $\text{ZnTPPI}$ , and  $\text{ZnTMPP}$  all follow the same trend. As for  $\text{ZnTPPE}$ , the HOMO is also mainly composed of  $\text{ZnTPP}$ , but the LUMO is almost composed of  $\text{ZnTPP}$  and E fifty–fifty. While for  $\text{ZnTPPG}$ , the LUMO are mainly composed of the acceptor G. The HOMO localizes at the donor moiety  $\text{ZnTPP}$  and the LUMO at the acceptor moieties for all the zinc metalloporphyrins selected, which agrees well with the energy demand of the molecular orbital for charge separation.

The energy levels of the molecular orbital from HOMO–5 to LUMO+3 of  $\text{ZnTPP}$  and the zinc metalloporphyrins selected are shown in Figure 5. Corresponding data of HOMO, LUMO, and HOMO–LUMO gaps are listed in Table 3. The energy gap between the HOMO and LUMO is 2.740 eV for  $\text{ZnTPP}$ . The energy gaps of the other molecules are all smaller than that of  $\text{ZnTPP}$ . The order of the energy gaps is  $\text{ZnTPPG}$  (2.194



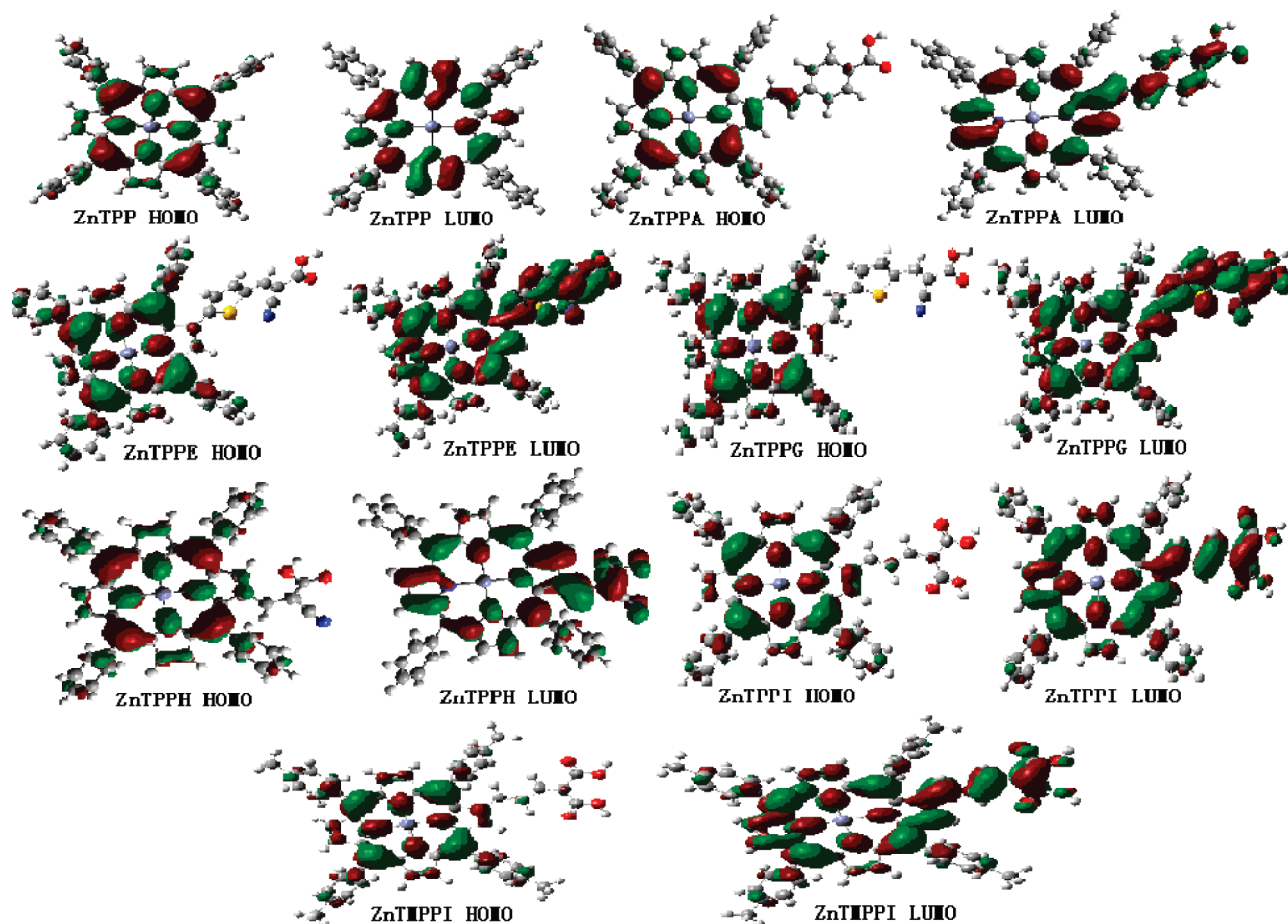


**Figure 4.** Molecular orbital distributions for ZnTPP and the zinc metalloporphyrins selected.

**TABLE 2: Percent Orbital Composition of ZnTPP and the Zinc Metalloporphyrins Selected**

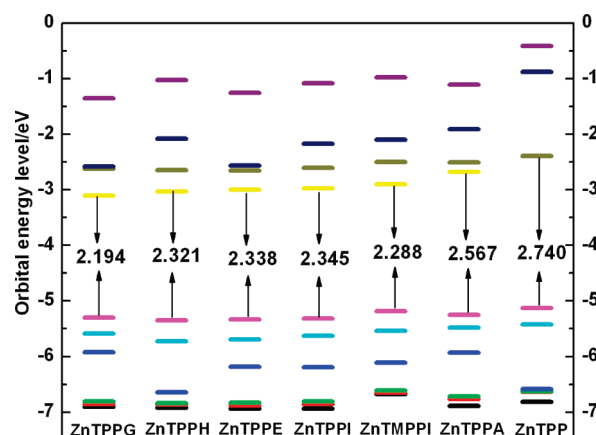
molecule	ZnTPPA		ZnTPPE		ZnTPPG	
	HOMO	LUMO	HOMO	LUMO	HOMO	LUMO
acceptor	3.0	18.6	0.33	58.8	1.25	72.0
COOH	0.17	2.83	0.01	7.1	0.06	7.0
CN					0.05	3.3
Zn	0.51	0.11	0.62	0.07	0.61	0.04

molecule	ZnTPPH		ZnTPPI		ZnTMPPI	
	HOMO	LUMO	HOMO	LUMO	HOMO	LUMO
acceptor	0.65	28.6	1.39	35.6	1.24	36.9
COOH	0.12	5.83	0.25	8.34	0.23	8.7
CN	0.07	2.62				
Zn	0.64	0.09	0.61	0.08	0.59	0.08

eV) < ZnTMPPI (2.288 eV) < ZnTPPH (2.321 eV) < ZnTPPE (2.338 eV) < ZnTPPI (2.345 eV) < ZnTPPA (2.567 eV) < ZnTPP (2.740 eV). The order of the photon-to-current conversion efficiencies reported in previous research works is ZnTMPPI (7.1%)<sup>16</sup> > ZnTPPH (5.2%)<sup>9</sup> > ZnTPPI (5.1%)<sup>16</sup> > ZnTPPA (4.11%).<sup>8</sup> It seems that to some extent the smaller the HOMO–LUMO gap of the sensitizer is, the higher the efficiency of corresponding solar cell is.

ZnTPPI and ZnTMPPI have the same acceptor, but ZnTMPPI has a higher HOMO and LUMO and a smaller energy gap than ZnTPPI owing to the additional electron-donating methyl group. It shows that the electron-donating ability of the composite methylphenyl group is stronger than that of a single phenyl group. ZnTPPG contains an additional unsaturated ethyl group and a longer conjugated chain as compared with ZnTPPE, which thus has a higher HOMO, lower LUMO, and a smaller energy



**Figure 5.** Orbital energy levels of ZnTPP and the zinc metalloporphyrins selected.

gap than those of ZnTPPE. It is also exciting to note that ZnTPPG has a lower energy gap as compared with ZnTMPPI. ZnTPPG may thus have a better performance as a solar cell sensitizer than ZnTMPPI according to the analysis above. That is to say, a conversion efficiency higher than the current record of 7.1% may be obtained for ZnTPPG-sensitized solar cells.

The HOMO and LUMO for ZnTPP are located at  $-5.131$  and  $-2.391$  eV, respectively. Similarly, the HOMO and LUMO of the other molecules were all lower than those of ZnTPP. For ZnTPP the LUMO and LUMO+1 are doubly degenerated but the other molecules were split. Compounds ZnTPPE, ZnTPPG, and ZnTPPH all contain electron-withdrawing cyan groups at the end, which decrease their LUMO and HOMO

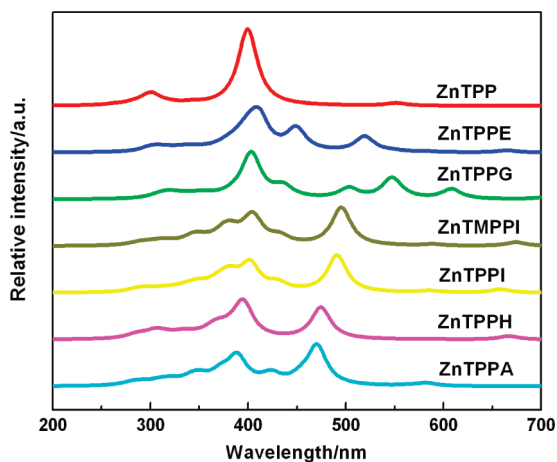
**TABLE 3: Orbital Energy Levels of ZnTPP and the Zinc Metalloporphyrins Selected**

orbital	$\epsilon_{\text{HOMO}}$	$\epsilon_{\text{HOMO-LUMO}}$	$\epsilon_{\text{LUMO}}$
ZnTPP	-5.131	2.740	-2.391
ZnTPPA	-5.249	2.567	-2.682
ZnTPPI	-5.318	2.345	-2.973
ZnTPPE	-5.336	2.338	-2.999
ZnTPPH	-5.350	2.321	-3.029
ZnTMPPI	-5.187	2.288	-2.898
ZnTPPG	-5.301	2.194	-3.108

energy levels and energy gaps as compared to ZnTPP. This shows that the electron-withdrawing cyan group plays an important role in tuning the properties of the sensitizer candidates.

**3.3. Electronic Absorption Spectra of Zinc Metalloporphyrin Complexes.** The calculated wavelengths, oscillator strengths, transition energies, and molecular orbital excitations for the most relevant transitions of the electronic absorption bands of ZnTPP and the selected zinc metalloporphyrins were obtained through TDDFT calculations in tetrahydrofuran (THF), which was often used in previous experimental research work. The electronic spectra were simulated by fitting to a Lorentzian line shape with a half-width at half-maximum of 12 nm. The simulated electronic spectra of ZnTPP and the selected zinc metalloporphyrins are shown in Figure 6. Corresponding wavelength, oscillator strength, transition energy, and molecular orbital excitation for ZnTPP and the zinc metalloporphyrins obtained from the TDDFT calculations are provided in the Supporting Information Table S1. The same trend of the Q-band positions of these complexes is observed as that of the HOMO–LUMO gaps from Kohn–Sham orbital energies shown in Figure 5, which further proves the validity of this approach.

All the metalloporphyrin compounds selected have more absorption bands than ZnTPP at the longer-wavelength side, as shown in Figure 6, which may be attributed to the longer conjugated chain or the thiophene ring in the acceptor section. ZnTPPG has the mostly red-shifted absorption bands among these compounds, which corresponds well with its smallest HOMO–LUMO gap. Comparing compounds ZnTPPI and ZnTMPPI shows they almost have the same figures in the electronic absorption spectra. The only difference is that ZnTMPPI has a slightly bathochromic shift to ZnTPPI, which corresponds well with the electron-donating effect of the additional methyl groups.

**Figure 6.** Electronic absorption spectra of ZnTPP and the zinc metalloporphyrins selected.

According to the previous observations,<sup>17</sup> if both donor and acceptor moieties have small HOMO–LUMO gaps, the donor–acceptor pairs would be more likely to have small HOMO–LUMO gaps, which likely further indicates higher conversion efficiency. The HOMO–LUMO gaps of many donor–acceptor combinations screened above are smaller than those of ZnTPPA and ZnTPPH, which have known highest cell efficiencies of 4.11%<sup>8</sup> and 5.6%<sup>9</sup> in simply substituted porphyrin-sensitized solar cells. And the HOMO–LUMO gap of ZnTPPG is even smaller than that of ZnTMPPI, which has the highest cell efficiency 7.1% in all porphyrin-sensitized solar cells.<sup>16</sup> This indicates that conversion efficiency challenging 7–8% may be obtained within the screened candidate ZnTPPG, which shows that the concepts of attribute axis and attribute coordinate system are very helpful in molecular property tuning and new molecule design. Further studies on the synthesis and characterization of these sensitizer candidates are in progress in our group.

Fortunately, a very recent publication<sup>21</sup> presented extensive spectroscopic and DFT studies as well as solar cell measurements of some porphyrin derivatives Ph, 1, 2, and 3, in which dye 1 corresponds to ZnTPPG in the current paper, indicating that attentions to the dyes with such structures are also paid by other researchers. Unfortunately, however, the dye 1 sensitized solar cell reported was not as efficient as expected,<sup>21</sup> which seems not to support the opinion and the molecule design strategy of the current paper. After detailed checking of that paper, some evidence is found that indicates the result reported is not the ideal performance of ZnTPPG. The very important data of those cells of compounds Ph, 1, 2 and 3, namely the fill factors, were not reported in that paper. They can be estimated to be 0.64 for compound Ph, 0.49 for compound 1, 0.49 for compound 2 and 0.60 for compound 3 from the  $V_{\text{oc}}$ ,  $J_{\text{sc}}$ , and  $\eta$  provided.<sup>21</sup> Such fill factors indicate obviously that those solar cells reported are still far from being optimized. As it is well-known in this field that the manufacturing process is an important factor that affects the final performance of the dye-sensitized solar cells, further optimization of the manufacturing process of those solar cells is thus still necessary before negating such a molecule design strategy.

#### 4. Conclusions

We present here the first example in which systematical design and screening of promising sensitizer candidates for DSSCs is possible assisted with the concepts of attribute axis and attribute coordinate system. Porphine and 11 kinds of bridge carbon substituted porphyrins as donors and 9 common acceptors A–I have been designed and calculated at the density functional B3LYP level. The substituent effects on the molecular orbital energy levels of the porphyrin derivatives have been discussed and promising donor–acceptor combinations are screened. Several novel zinc metalloporphyrins selected were then calculated by means of DFT/TDDFT method in THF solvent. The electronic and spectroscopic properties of ZnTPP and the selected novel zinc porphyrin complexes have been investigated and compared with previous experimental works. The results show that the candidates selected are very promising to provide better performances as sensitizers. Substituents with different electron-withdrawing or -donating abilities along the corresponding attribute axis can be used to systematically tune the molecular orbital energy levels of porphyrins in a wide range, and thus, further, the charge transfer orientation may be controlled and designed. This rational design method supplies an unique predictive power over these systems and may also be extended to other functional molecules.

**Acknowledgment.** We thank the National Natural Science Foundation of China (20501011) and Liaocheng University (31805) for financial support.

**Supporting Information Available:** Calculated wavelength, oscillator strength, transition energy, and molecular orbital excitations for ZnTPP and the zinc metalloporphyrins. This material is available free of charge via the Internet at <http://pubs.acs.org>.

## References and Notes

- (1) Huang, S.; Deng, H.; Lan, M. *Chem. Phys. Trans.* **1997**, *10* (2), 150.
- (2) Grätzel, M. *J. Photochem. Photobiol. C* **2003**, *4*, 145–153.
- (3) Robertson, N. *Angew. Chem., Int. Ed.* **2006**, *45*, 2–10.
- (4) Kong, F. T.; Dai, S. Y.; Wang, K. J. *Adv. Optoelectron.* **2007**, 75384.
- (5) Hamann, T. W.; Jensen, R. A.; Martinson, A. B. F.; Ryswyk, H. V.; Hupp, J. T. *Energy Environ. Sci.* **2008**, *1*, 66–78.
- (6) Nazeeruddin, Md. K.; De Angelis, F.; Fantacci, S.; Selloni, A.; Viscardi, G.; Liska, P.; Ito, S.; Takeru, B.; Grätzel, M. *J. Am. Chem. Soc.* **2005**, *127*, 16835.
- (7) Campbell, W. M.; Burrell, A. K.; Officer, D. L.; Jolley, K. W. *Coord. Chem. Rev.* **2004**, *248*, 1363–1379.
- (8) Nazeeruddin, Md. K.; Humphry-Baker, R.; Officer, D. L.; Campbell, W. M.; Burrell, A. K.; Grätzel, M. *Langmuir* **2004**, *20*, 6514–6517.
- (9) Wang, Q.; Campbell, W. M.; Bonfantani, E. E.; Jolley, K. W.; Officer, D. L.; Walsh, P. J.; Gordon, K.; Humphry-Baker, R.; Nazeeruddin, Md. K.; Grätzel, M. *J. Phys. Chem. B* **2005**, *109*, 15397.
- (10) Schmidt-Mende, L.; Campbell, W. M.; Wang, Q.; Jolley, K. W.; Officer, D. L.; Nazeeruddin, Md. K.; Grätzel, M. *ChemPhysChem* **2005**, *6*, 1253–1258.
- (11) Rai, S.; Ravikan, M. *Tetrahedron* **2007**, *63*, 2455.
- (12) Flamigni, L.; Ventura, B.; Tasior, M.; Gryko, D. T. *Inorg. Chim. Acta* **2007**, *360*, 803.
- (13) Wienke, J.; Schaafsma, T. J. *J. Phys. Chem. B* **1999**, *103*, 2702.
- (14) Kroeze, J. E.; Savenije, T. J.; Warman, J. M. *J. Photochem. Photobiol. A* **2002**, *148*, 49.
- (15) Wamser, C. C.; Kim, H.-S.; Lee, J.-K. *Opt. Mater.* **2002**, *21*, 221.
- (16) Campbell, W. M.; Jolley, K. W.; Wagner, P.; Wagner, K.; Walsh, P. J.; Gordon, K. C.; Schmidt-Mende, L.; Nazeeruddin, Md. K.; Wang, Q.; Grätzel, M.; Officer, D. L. *J. Phys. Chem. C* **2007**, *111*, 11760.
- (17) Balanay, M. P.; Dipaling, C. V. P.; Lee, S. H.; Kim, D. H.; Lee, K. H. *Solar Energy Mater. Solar Cells* **2007**, *91*, 1775–1781.
- (18) Zhang X. Ph.D. Thesis, Shandong University, Jinan, China, 2004.
- (19) Frisch M. J. et al. *Gaussian'03*, revision B.05, Gaussian, Inc.: Pittsburgh, PA, 2003.
- (20) Mizuseki, H.; Niimura, K.; Majumder, C.; et al. *Mol. Cryst. Liq. Cryst.* **2003**, *406*, 11/[205].
- (21) Lind, S. J.; Gordon, K. C.; Gambhir, S.; Officer, D. L. *Phys. Chem. Chem. Phys.* **2009**, *11*, 5598–5607.

JP905412Y